*Iranian Journal of Hydrogen & Fuel Cell 4(2017) 307-321*

Iranian Journal of Hydrogen & Fuel Cell

**IJHFC**

Journal homepage://ijhfc.irost.ir

# Sulfurous analysis of bioelectricity generation from Sulfate-Reducing Bacteria (SRB) in a microbial fuel cell

**M. Rahimi[1], S.M. Sadrameli[1,*], H. Mohammadpoor[1], H. Kazerouni[2], M.D. Ghaffari[3]**

[1] Department of Process Engineering, Faculty of Chemical Engineering, Tarbiat Modares University, Tehran, Iran
[2] Department of Chemical Engineering, Biotechnology group, Amirkabir University of Technology, Tehran, Iran
[3] Microbiology Group, Shahed University, Tehran, Iran

**Article Information**

Article History:

Received:
26 Dec 2017
Received in revised form:
21 May 2018
Accepted:
24 May 2018

**Keywords**

Microbial Fuel Cell (MFC)
Electrode
Bacterial growth
Sulfate-Reducing Bacteria (SRB)

**Abstract**

The current importance of energy emphasizes the use of renewable resources (such as wastewater) for electricity generation by microbial fuel cell (MFC). In the present study, the native sulfate-reducing bacterial strain (R.gh 3) was employed simultaneously for sulfurous component removal and bioelectricity generation. In order to enhance the electrical conductivity and provision of a compatible bed, a complex electrode structure based on stainless steel-304 was prepared. Next, the electrode was coated with a composite of graphite and activated carbon solution. A new approach associated with increasing bacterial population was studied using two electron acceptors composed of iron and sulfate for respiration of sulfate-reducing bacteria. Finally, according to the maximum living cell number (nM = 20 $\times 10^8$ cell ml-1) and the conditions of the bioreactor including the highly efficient anode electrode, a higher current generation (2.26 mA for the new structure as compared to 1.73 and 1.29 mA for graphite rod and carbon paper, respectively) was observed in the culture media.

## 1. Introduction

Microbial fuel cells (MFCs) can be used in the treatment of wastewater to produce electricity [1], they can also in some cases be applied in diagnostic applications for monitoring and sensing [2]. The microorganism acts as a biocatalyst in the biofuel generation process [3, 4]. Although it seems that

*Corresponding Author's Fax: +98 21 82884902
E-mail sadrameli@modares.ac.ir

doi: 10.22104/ijhfc.2018.2684.1161

the presence of sulfate-reducing bacteria (SRB) are undesirable due to the generation of significant toxic and odorous hydrogen sulfide [5], however ecological and economic advantages associated with SRBs make them a very good option for industrial processes [6]. (make sure I did not change your meaning) The existence of many kinds of SRB in various wastes discharged into the environment makes them difficult to use for industrial purposes [7]. Production of sulfide by SRB creates serious problems associated with corrosion [8] in the petroleum and other industries [9]. Sulfate is the most oxidized state of sulfur and accounts for its most stable form [10]. Also, since sulfate is the most dominant anion in natural water [11] it can be used by SRBs as a source of energy and a terminal electron acceptor. Different enriched microbial communities are found on a microbial fuel cell during sulfide oxidation; and various materials used for it structure, such as the composite of activated carbon cloth and carbon-fiber veil[12], have been widely used to improve the performance of such systems [13].

Nevertheless, surface non-uniformity and pore size cause problems of clogging and the demise of bacteria in long-term operations [14]. Good conductivity and cell adhesion to the surface play an important role in power generation [15]. Hence, research has concentrated on finding new structures that have good conductivity and low resistance to transfer of electrons as well as high-quality toughness and excellent bio-compatibility for bacterial activity [16]. Using metal as the electrode material is an expedient option to reduce the operational cost of MFC [17]. Metals such as stainless steel mesh (SSM) and stainless steel fiber felt (SSFF) have been employed to provide a 3D support and at the same time act as an anodic current collector of the MFC. Although the metal based fiber possesses high strength, conductivity, and resistance to corrosion, its poor biocompatibility and large over-potential hinder its wider application in MFC. Therefore, the performance of SSFF has been improved via modification with either GR, CNT or AC through binder-assisted pasting. Table 1 summarizes the performance of MFCs operated with modified SSM as the anode electrode.

In the present work, stainless steel-304 (which has high conductivity) combined with graphite and activated carbon powders (that provide adhesion) were introduced as a new structure for microbial fuel cells in a medium-enriched with SRBs. Stainless steel-304 with a pore size of 250 μ was employed as the base of the anode electrodes. Problems associated with electrode structure, such as cells lost over a period of time (because of clogging and fouling), and easy production for scale up issues were also analyzed in the new electrode design.

Moreover, the effect of the number of living cells on sulfide generation was investigated for the first time. Also, fluctuation of some special ions in the SRB culture medium, such as sulfate ferrous, and their influence on other definitive factors was assessed in MFCs enriched with SRBs.

## 2. Materials and methods

### 2.1 Materials

Stainless steel coupons with dimensions of 20 mm×10 mm were purchased from a local market in Tehran, Iran. The percent weight composition measured by a XRF apparatus (PW- 2404, Philips) was 12.6745 Cr, 1.375 Mn, 66.373 Fe, 10.609 Ni and 8.968 Cu. Carbon paper (CP) was purchased from MAST Carbon Advanced Products Ltd., UK and a commercially available graphite rod (GR) was obtained from SGL Technologies GmbH, Germany. The proton exchange membrane (PEM), Nafion-117, was supplied by the DuPont Company, USA.

### 2.2 Electrode preparation

The stainless steel coupons (pore size 250 μ) were rinsed 100% with acetone in order to eliminate any grease on them. Then, a composite of graphite powder (1.2 mg $cm^{-2}$), activated carbon (1.2 mg $cm^{-2}$), 2-propanol (65% v/v), deionized water (35% v/v) and conductive glue (0.20 mg $cm^{-2}$) were put in an

**Table. 1. Performance of MFC with stainless steel as the anode base structure**

| Authors | Bacteria/ biocatalyst source | Carbon source | Anode material | Performance |
|---|---|---|---|---|
| Song et al. [35] | Anaerobic sludge | Artificial waste water with acetic acid | SSM/EGR-SDS | SSM/EGR-SDS-MWCNT (1640 mW/m$^2$), SSM/EG-MWCNT (1369 mW/m$^2$) |
| Hou et al. [36] | Domestic waste water | Sodium acetate | SSFF-CNT | SSFF-CNT (1280 mW/m$^2$) |
| | | | SSFF-GR | SSFF-GR (2142 mW/m$^2$) |
| | | | SSFF-AC | SSFF-AC (560 mW/m$^2$) |
| | | | SSFF | SSFF (0.8 mW/m$^2$) |
| Zheng et al. [37] | Mixed culture | Artificial waste water with acetate | SSM/carbon black | 3215 mW/m$^2$ |
| Guo et al. [38] | *Geobacter sp.* | Sodium acetate | SS-Felt | SS-Felt (27.42 mA/cm$^3$) control (0.85 mA/cm$^3$) |
| Lamp et al. [39] | Anaerobic digester | Glucose | SSM-CNS | SSM-CNS (187 mW/m$^2$) SSM (3 mW/m$^2$) |
| Erbay et al. [40] | *Shewanella oneidensis* | Truptic soy broth | SSM-CNT | SSM-CNT (450 mW/m$^2$) SSM (0.48 mW/m$^2$) |

ultrasonic bath for 30 min to mix uniformly and also vaporize the solvent. After that, the reticular stainless steel coupon base of the electrode was coated with the above solution by an Air-Brush KIT (model BD-116c) connected to a compressor with 1.2 bar at 20°C. Afterward, the plate was placed in the oven and baked at 250°C for 1 h. Determination of electrochemical behavior was performed by a cyclic voltammetry test [18] on three different electrodes (stainless steel-304, activated carbon, and graphite powder (SsCG), graphite rod (GR) and carbon paper (CP)).

### 2.3. MFC set-up and operation conditions

A two-compartment MFC (Fig. 1) was constructed of Plexiglas with a working volume of 48 ml. The SsCG electrode was cut into two 2 cm × 1 cm pieces. Both electrodes were connected to a long titanium wire (1.2 mm thickness) to facilitate the passage of current. Nafion-117 (PEM, DuPont) with 4 cm$^2$ projected surface areas was used as the proton exchange membrane. Two bioreactors, one placed in a shaker and the other in an incubator (90 rev min$^{-1}$), were used at the same time. The temperature was adjusted to 30°C and $O_2$ was removed by $N_2$ sparging for 30 min before beginning the operation. The pH of the solution was kept at 7.47 as optimum pH for bacterial growth. Phosphate buffer solution consisting of (per liter): KCL 0.1 g, NaCl 4 g, $Na_2HPO_4$ 0.72 g and $KH_2PO_4$ 0.1 g was used in all the experiments. Three artificial wastewater samples were prepared with different concentrations of $FeSO_4$: Culture M (moderate concentration) consisted of 1 g cm$^{-3}$ $FeSO_4$, equivalent of 3.6 mmol cm$^{-3}$ $Fe^{2+}$; Culture H (high concentration) with 3 g cm$^{-1}$ $FeSO_4$, equivalent of 10.8 mmol cm$^{-3}$ $Fe^{2+}$; and Culture L (low concentration) which served as the control medium without any $FeSO_4$. $SO_4^{2-}$ content, a vital factor in a culture medium, was 15.48, 19.08, and 26.27 mmol cm-3 for samples L, M and H, respectively. It should be noted that the base of the culture medium in these three artificial wastewater was composed of yeast extract 1 g l$^{-1}$, $KH_2PO_4$ 0.5 g l$^{-1}$, $CaSO_4$ 1 g l$^{-1}$, $Na_2SO_4$ 1 g l$^{-1}$, $NH_4CL$ 1 g l$^{-1}$, $MgSO_4.7H_2O_2$ g l$^{-1}$, $FeSO_4.7H_2O$ 0.5 g l$^{-1}$ and ascorbic acid 0.1 g l$^{-1}$. Carbon source was used for the culture medium as initial chemical oxygen demand (COD) and sodium lactate 50% with a concentration of 7.79 g cm$^{-3}$ was injected into all the culture media. Initial pH was regulated at 7.46 (pH was adjusted to 7.46 at all times because at a pH less than 7 $H_2S$ is the most dominant inhibitor and also reduces the loss of volatile $H_2S$). Bacterial

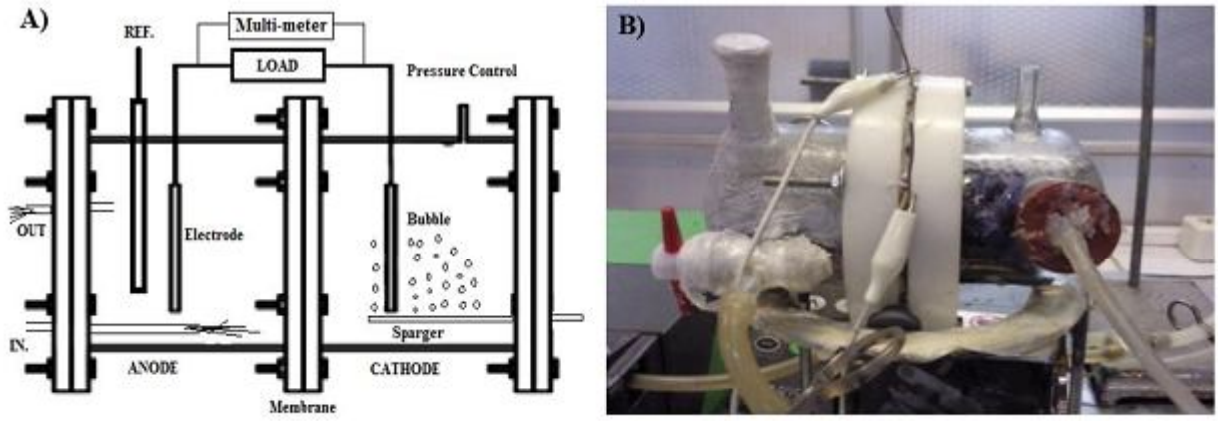


**Fig. 1. a) Schematic representation of the two-compartment MFC, b) The picture of the two-compartment MFC system.**

inoculation ($2.5\times10^6$ cell $ml^{-1}$) was done at the beginning of each experiment. Then, the bacterial medium was incubated on bioreactors and inserted into the shaker and incubator (30°C, 90 rev $min^{-1}$).

### 2.4. Electrochemical measurements

Potentiostatic measurement (Ivium, Netherlands) was performed using three electrode systems connected to personal computer software. A reference electrode of Ag/AgCl + Pt EI (IRI.2000-E which had +196 mV versus NHE) was used in the potentiostatic experiment.

### 2.5. Isolation of the SRB strains

Three different types of SRBs isolated from cooling water, river area and urban wastewater were SRB strains R.gh 1, R.gh 2, and R.gh 3, respectively. The bacterial strains were isolated from the SRB agar medium (sodium lactate 0.5 g $l^{-1}$, yeast extract 1 g $l^{-1}$, $KH_2PO_4$ 0.5 g $l^{-1}$, $Na_2SO_4$ 1 g $l^{-1}$, $NH_4CL$ 1 g $l^{-1}$, $MgSO_4.7H_2O$ 2 g $l^{-1}$, $CaCL_2.6H_2O$ 1 g $l^{-1}$, $FeSO_4{\cdot}7H_2O$ 0.5 g $l^{-1}$, ascorbic acid 0.1 g $l^{-1}$, Agar-Agar 15 g $l^{-1}$, pH = 7.4). The open-circuit potential was recorded in the culture medium (sodium lactate 0.5 g $l^{-1}$, yeast extract 1 g $l^{-1}$, $KH_2PO_4$ 0.5 g $l^{-1}$, $CaSO_4$ 1 g $l^{-1}$, $Na_2SO_4$ 1 g $l^{-1}$, $NH_4CL$ 1 g $l^{-1}$, $MgSO_4.7H_2O$ 2 g $l^{-1}$, $FeSO_4.7H_2O$ 0.5 g $l^{-1}$, ascorbic acid 0.1 g $l^{-1}$ and pH = 7.46 [19]. After inoculation, the culture medium was incubated at 30°C for 5 days. Finally, bacterial strain R.gh 3 obtained from urban wastewater was selected as the best strain for this study because of its maximum open circuit potentiates in the series of batch design (370 mV for R.gh 3 versus 240 mV for R.gh 1 and 210 mV for R.gh 2 in the early evaluation).

### 2.6. Microscope observation

The electrode structure, electrocatalytic activity and cell adhesion strengths are the major parameters in a microbial fuel cell [20]. A metallographic microscope (OLYMPUS-DP25, Japan) was used to verify the uniformity of electrode coatings. The cell community (dead and live) was observed using a fluorescence microscope [21] (MOTIC, FITC LENS, EX D480/30x, DM 505DCLP, BA D535/40m) on the electrode surface. Acrydin orange (A.O.) fluorescence dye was utilized for cell observation. For staining, the electrodes were dipped in a solution containing fluorescence dye (A.O. 0.01 mg, formaldehyde 5.4 ml and 94.6 ml deionized water) for 15 min in a dark chamber.

### 2.7. Colony forming unit (CFU $ml^{-1}$)

In order to assess the viability of the bacteria present in the anode chamber at different times of the operation, CFU $ml^{-1}$ versus time was used [22]. Numeration cells were counted at 1000x magnification by means of a colony counter (Stuart - SC6). An average of 30

plates was chosen as the number of viable bacteria present in the sample. The buffer used for this analysis was comprised of (per liter): NaCl 8 g, KCl 0.2 g, $Na_2HPO_4$ 1.44 g and $KH_2PO_4$ 0.24 g.

### 2.8. Analysis of sulfurous components

The amount of dissolved sulfide in the culture medium was measured by deposition of colloidal CuS in copper sulfate reagent [23]. Determination of sulfate, sulfite and thiosulfate anions was done using HPLC (KNAUER, RF-10AXL) analysis at different time intervals. Liquid chromatographic determinations of anions were done with an ultraviolet (307 nm) detector at room temperature. Samples from the reactor were collected and filtered using a syringe filter with a pore size 0.45 µm prior to the test. Injections were made from either 10 µl or 100 µl loops. The columns, tubes and conductivity detector were insulated well to ensure constant temperature. The eluent used as buffer in this case was $Na_2CO_3$ (3.5 mmol $l^{-1}$) + $NaHCO_3$ (1.0 mmol $l^{-1}$).

### 2.9. Determination of ferric and ferrous ions

A spectrophotometer (JENWAY, 6310) was used to determine $Fe^{3+}$ and $Fe^{2+}$ cation in the solution. In order to analyze $Fe^{3+}$, 0.1 ml culture liquid was blended with 3 ml 5-sulfosalicylic acid 10% (v/v). Then, 97 ml deionized water was added to the mixture until the volume reached 100 ml. Finally, absorbance was recorded at a 500 nm wavelength. To determine Fe, 3 ml of ammonium hydroxide 25% was added to the previous solution and absorbance was quickly measured at 425 nm. The difference between the total and ferric iron is the ferrous concentration in the solution [24].

## 3. Results and discussion

### 3.1. Electrocatalytic behavior of electrodes in the absence of bacteria

A phosphate buffer solution as a base medium was employed in the MFC to evaluate the electrode characterization. As is shown in Fig. 2, the SsCG electrode has a larger current response as compared to the GR and CP. This is a result of the enhanced surface area of SsCG. The scan range was adjusted between -0.8 V and -0.4 V in the absence of bacterial culture. The maximum current generation reached was 1.06, 0.62 and 0.58 mA for SsCG, GR and CP at a voltage of -0.3, -0.34 and -0.13 V, respectively,

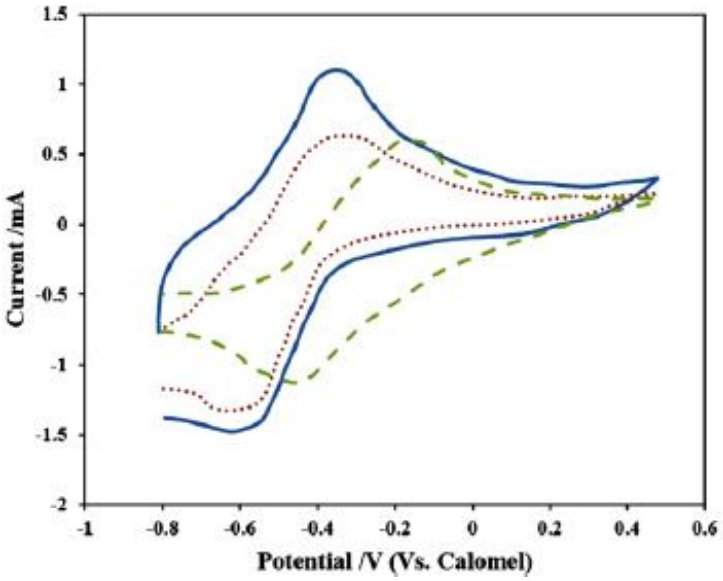


**Fig. 2. CVs of SsCG (solid line), GR (dotted line) and CP (dash line) in the buffer solution.**

in the oxidation reaction. Moreover, the proximity of the peaks in the SsCG curve, i.e., the anodic and cathodic peak potentials, confirm that the reversible oxidation-reduction reaction occurred. This plays an important role in increasing the electroactive surface area.

### 3.2. Electrical resistivity

Two parallel probes were used for the electrical assessment of the electrodes [25]. As shown in Table 2, electrical conductivity of SsCG is nearly ten times greater than that of the activated carbon cloth. Using stainless-steel 304 with high conductivity ($\sigma$=1.38×10$^4$ S cm$^{-1}$) as the base for the electrode has the crucial effect of greater capability to facilitate electron transfer. Moreover, a linear increase in conductivity was observed up to a certain amount of active carbon in the coating. The lower resistance of the electrode reduces the internal resistance of the bioreactor, which is one of the major limits to electron transfer across the load [26].

### 3.3 Electrode capacity

The capability to adsorb sulfur deposition via sulfide oxidation on the electrode surface decreases over time [13]. Therefore, the level of electrical activity is also reduced. In order to examine the electron transfer capability of SsCG, potentiostatic analyses were performed at a constant potential of 0.30 V against Ag/AgCl. The maximum current level of 2.5 mA cm$^{-2}$ was quickly recorded after adding 5 mM (mmol l$^{-3}$) sulfide to the buffer solution in the first cycle of the operation (Fig. 3). After 15 h the minimum level of sulfide concentration was obtained, which confirmed the almost proper adsorption of sulfide on the electrode surface. The same concentration was added to the buffer in the following cycles. In the fourth cycle upon adding sulfide (total of 20 mM) the current density reached a maximum of 2.14 mA cm$^{-2}$, which was two times greater than CP (0.98 mA cm$^{-2}$ in the first cycle, data not shown) and one and half times greater than GR (1.21 mA cm$^{-2}$ in the first cycle; data not shown). After eight cycles of operation, the 4 cm$^2$ surface of the mentioned electrode showed a 30% reduction of absorbance (according to sulfide concentration in the buffer), which demonstrates the excellent performance of this new structure in the media.

### 3.4. Electrode assessment in the presence of bacteria

Fig. 4 presents the CVs test for SsCG, GR and CP after inoculation with SRB bacteria. There was a

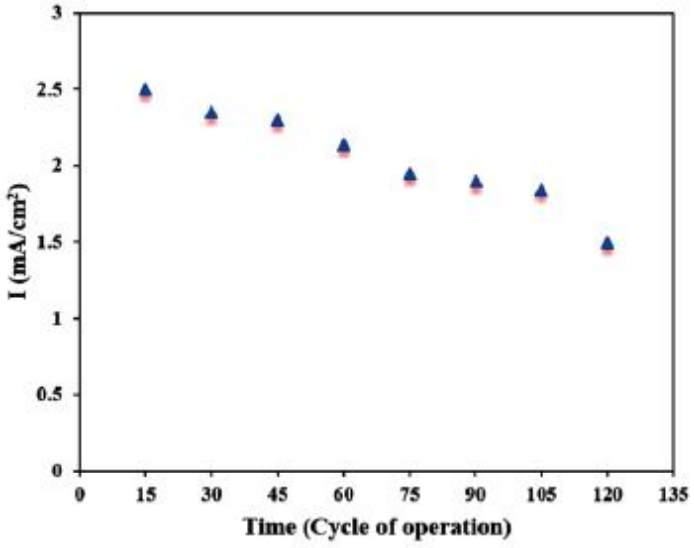


**Fig. 3. Long-term stability of current generation by SsCG electrode.**

**Table. 2. Electrical conductivity of various electrode structure materials**

| Conductivity (S $cm^{-1}$) | Electrode |
|---|---|
| 0.5 – 0.85 | Stainless steel-304 plus activated carbon plus graphite powder (SsCG) |
| 0.075 | Carbon paper (CP) |
| 0.055 | Graphite rod (GR) |
| 0.070 [13] | Activated carbon cloth |

peak of 2.26 mA at 0.15V in the oxidation scan and a peak of -1.2 mA at -0.48 V in the reduction scan. The current peaks were recorded as 1.73 and 1.29 mA for CR and CP, respectively, which are lower than that of SsCG. This can be attributed to the quick transference of electrons across the SsCG electrode as compared to other electrodes. Separation of the two peaks in the SsCG electrode is smaller than that of the other two electrodes. Thus, it was confirmed that activated carbon plus stainless steel-304 plays an important role in activating the surface in terms of electrocatalytic activity.

### 3.5. Morphology and bioelectrocatalytic characterization

Fig. 5 depicts two sides of the SsCG electrode coupons (A, A´ and B, B´ indicate the upper and lower surfaces, respectively) and the other electrodes with an appropriate experiment using the fluorescence test (SsCG (E), CP (F) and GR (G)). Despite the fact that use of GR and CP electrodes is prevalent worldwide, issues associated with clogging, fouling and loss of the active layer for mass transfer by living cells in the biofilm on electrode surface are unavoidable. On the other hand, the more active biofilm adhered on the surface the more electron transfer and as a result the greater current level in the MFCs. Thus, surface property was scrutinized after 30 days of operation in the bioreactor. According to Fig. 5, the number of living cells (bright spots) on the greater current level in the MFCs. Thus, surface property was scrutinized after 30 days of operation in the bioreactor. According to Fig. 5, the number of living cells (bright spots) on the SsCG electrode surface (E) is more than that of CP (F) and GR (G). Integration of living cells and the number of active bacterial cells on the surface of the SsCG electrode are more than that of the others, as shown by yellow circles in the figure. The excessive amount of pores which exist in some commercial materials, such as carbon paper, may lead to the death of some cells as well as reduce the active surface of the electrode reaction [27]. In other words, adhesion strength and as a result bioelectroactivity was observed in a long-term operations, which influences the performance of the microbial fuel cells.

### 3.6. Effect of ferrous sulfate on bacterial growth

According to previous studies, the presence of ferric ion in a solution has a close relationship with the bacterial growth of sulfate-reducing bacteria as well as an increasing the number of active-living cells [28]. Additionally, in some cases an increase of sulfate ferrous in the culture medium has no significant effect on the duplication of bacteria [29]. With the presence of $Fe^{2+}$, this ion might be oxidized to $Fe^{3+}$ and act as the terminal electron acceptor for respiration of bacteria [30]. According to Fig. 6, the number of living cells increased faster to a maximum value in medium H ($n_H = 19.8\times10^8$ cell $ml^{-1}$)
as compared to the other mediums during the 24 h operation. The maximum number of bacteria with a as well as reduce the active surface of the electrode reaction [27]. In other words, adhesion strength and as a result bioelectroactivity was observed in a long-term operations, which influences the performance of the microbial fuel cells.

### 3.6. Effect of ferrous sulfate on bacterial growth

According to previous studies, the presence of ferric ion in a solution has a close relationship with the bacterial growth of sulfate-reducing bacteria as

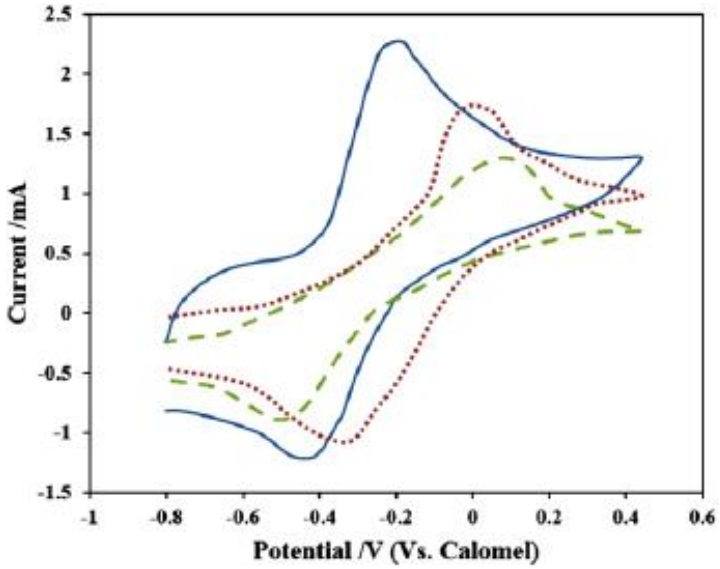


**Fig. 4. CVs of the SsCG (solid line), GR (dotted line) and CP (dash line) in the presence of bacteria.**

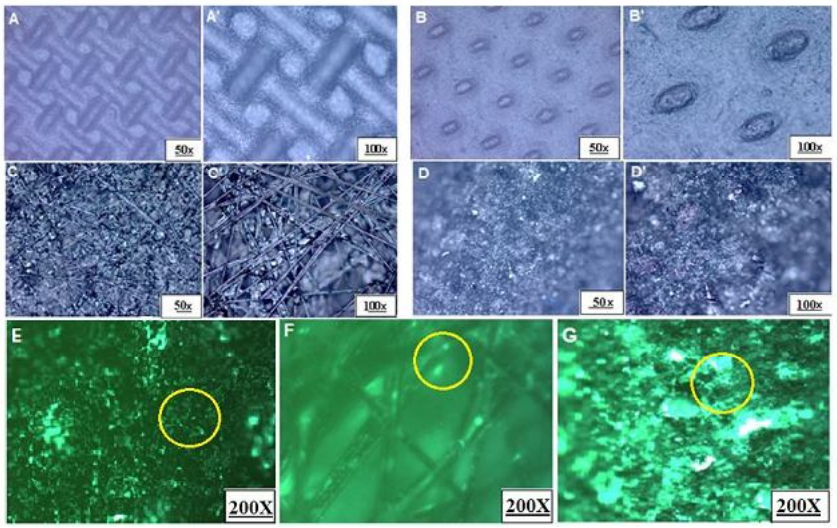


**Fig. 5. Metalography of SsCG up (A, A´) and down (B, B´), CP (C, C´), GR (D, D´) of the surface. Living cells of SsCG (E), CP (F) and GR (G) after operation in MFC using fluorescence analysis.**

well as an increasing the number of active-living cells [28]. Additionally, in some cases an increase of sulfate ferrous in the culture medium has no significant effect on the duplication of bacteria [29]. With the presence of $Fe^{2+}$, this ion might be oxidized to $Fe^{3+}$ and act as the terminal electron acceptor for respiration of bacteria [30]. According to Fig. 6, the number of living cells increased faster to a maximum value in medium H ($n_H$ = 19.8×10$^8$ cell ml$^{-1}$) as compared to the other mediums during the 24 h operation. The maximum number of bacteria with a 24 h delay for sample M reached $n_M = 20\times10^8$ cell ml$^{-1}$, while the maximum value reached nL= 19.92×10$^8$ cell ml$^{-1}$ after 62 h of operation for the control sample without any sulfate ferrous. Finally, after 10 days the number of living cells diminished to their lowest amounts of $n_H = 3.46\times10^8$, $n_M = 4.5\times10^8$, and $n_L = 7.3\times10^8$ cell ml$^{-1}$. However, the amount of $Fe^{3+}$ ion in Fig. 7 indicates that the main fluctuations occurred in sample H. As can be seen in Fig. 7, concentration of $Fe^{3+}$ ion reached 6.74 mmol cm$^{-3}$ in the first 10 h, 3.53 mmol cm$^{-3}$ in 24 h, and 1.12 mmol cm$^{-3}$ in

48 h. At the same time, with this increase a decrease of $Fe^{2+}$ from 10.79 to 3.12 mmol $cm^{-3}$ in the initial 10 h was observed. Afterward, concentration of $Fe^{2+}$ increased to a fixed value of 7.4 mmol $cm^{-3}$ at 140 h, which confirmed the redox reaction activity of this ion in the culture media. Again, variation in the rate of $Fe^{3+}$ (Fig. 7) shows weaker activity in solution M where the amount of ferric ion reached a maximum value of 2.59 mmol $cm^{-3}$ in 24 h then decreased to 0.1 mmol $cm^{-3}$ at 140 h. Therefore, it is revealed that the maximum consumption and formation of the ferric ion were observed in medium H. As was shown in Fig. 6, cells growth increased noticeably with the enhancement of ferric ion in the culture medium because bacteria can choose $Fe^{3+}$ as a final electron acceptor for respiration in the chain [31]. As a result, the portion consumption of the $Fe^{3+}$ ions is directly related to the increasing bacterial living cells number. In addition, material such as $Ni^{2+}$ which exists in the base of designed electrode (SsCG) can also have great impact on duplication of living cells [29].

Sulfate, as a source-specific of SRBs in respiration,

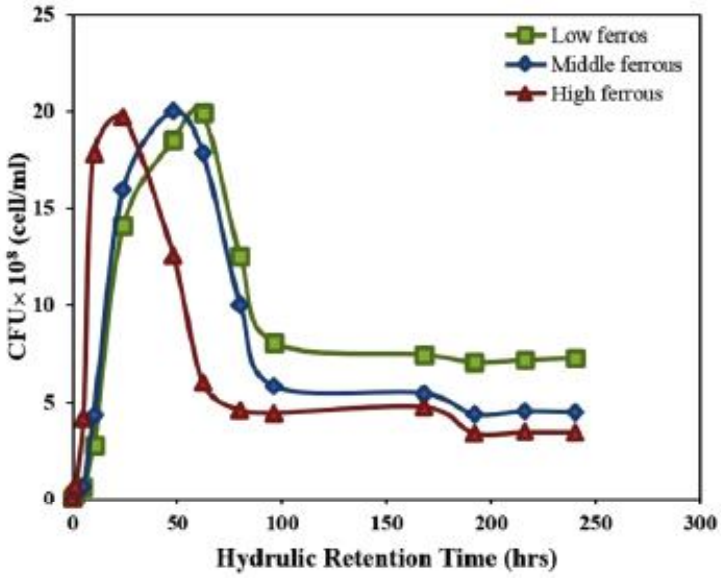


**Fig. 6. Effect of various sulfate iron concentration on the number of living cells in anode compartment vs. HRT.**

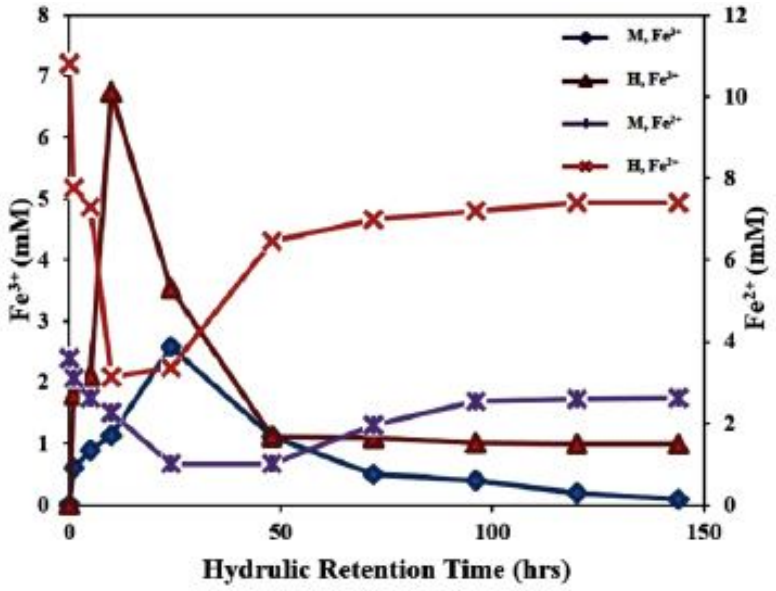


**Fig. 7. Variation of ferric and ferrous ions against hydraulic retention times in different concentrations of sulfate iron.**

can also be used as a terminal electron acceptor in the respiratory chain [32]. Large consumption of $SO_4^{2-}$ by SRB has a very important effect on the number of living cells (slope of the curve for medium H in Fig. 8 is lower than that of mediums M and L). As is shown in Fig. 8, biological sulfide generated by SRBs reached 10.74 mM in 24 h with more sulfides in comparison with culture M with 6.34 mM and culture L with 4.33 mM. Furthermore, as the biologically produced sulfide increases, the number of living cells increases. It must be pointed out that the existence of ferric ion in the initial hours in the medium has a positive effect on the rate of manifolding of cells.

Fig. 9 shows a greater reduction of chemical oxygen demand (COD) in medium H as compared to the others. The rapid decline of bacterial carbon source is proportional to the multiplication of bacterial population [33]. Hence, tangible enhancement can be expected on the final metabolism as well as open circuit potential. As it is observed in Fig. 9, the carbon source is depleted by 33% in the H solution as compared to 31 and 25% in the M and L media in the first 24 h, this indicates that SRB has consumed a larger amount of the carbon source in the H solution. Then, a reverse of the changes was observed at 48 h when the carbon source in the L solution diminished more than the other media. This may be due to a severe reduction in COD for the H medium in the early hours and a greater number of viable bacteria in the L solution from this time onwards in accordance with Fig. 6. Finally, after 192 h of bioreactor operation, 74, 67 and 63% COD removal was observed for L, M and H solutions, respectively. There are two interesting features which can be deduced from Fig. 9: First, appropriate removal of COD was observed in the presence of SRBs by the MFC reactor. Second, the correct view of bacterial activity was offered in order to remove the carbon source. For instance, one of the reasons for the steep decline in COD removal is due to the abundance of a large amount of ferrous ions ($Fe^{2+}$) in the H media causing partial deposition of ferrous as FeS [34]. This affects the bacterial activity in the solution, as a result less carbon source is consumed. It is also revealed that there is a significant interaction and competition between the use of $Fe^{2+}$ and $SO_4^{2-}$ in the presence of SRBs, this can be optimized in a future study.

### 3.7. Effect of biofilm formation on electron transfer and exoelectrogenic activity

Bacterial cells that can attach to the surface and create continuous biofilm play an important role in the performance of MFCs. Although, sulfide concentration is the dominant-control on potential in short-term operations, active layer adhesive on

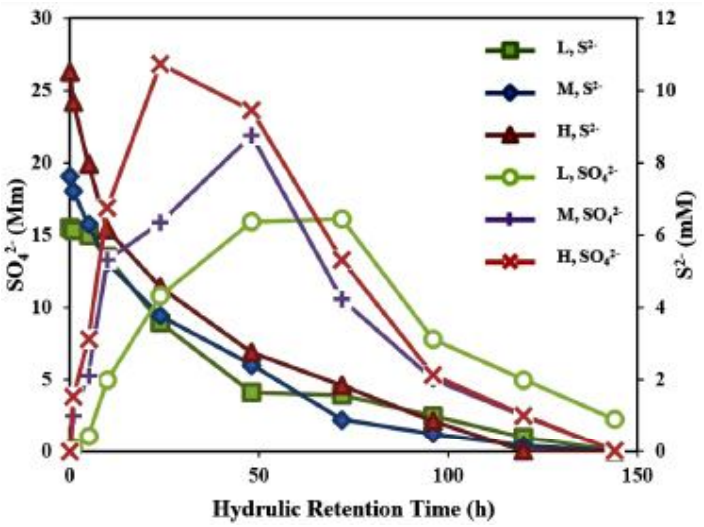


**Fig.8. Changes in sulfate (left side of the curve) and sulfide (right side of the curve) ions in different media containing ferrous sulfate vs. HRT.**

the surface also has a crucial effect on electron transfer in long-term operations. In order to clarify the capability of electron transfer by SRB to the electrode, definitive living cells ($2.5\times 10^6$ cell $ml^{-1}$) were injected into the anode chamber without any iron sulfate as a terminal electron acceptor. Projected-surface area of the electrode was 4 $cm^2$ with 50 $cm^3$ as working volume. Sodium lactate (with a concentration of 4 g $l^{-1}$)
was used as the electron donor in each step of the test. The anode electrode was poised at 300 mV by potentiostatic to regulate the bacterial activity. Fig. 10 shows continuous current generation versus time in three steps of the operation. In the first step, after injection of sodium lactate as the sole electron donor the current level increased to a maximum of 0.83 mA $cm^{-2}$. Then, as the carbon source reduced in the medium the current level decreased over time. Re-injection of sodium lactate as the sole electron donor led to an increase in the current to 0.86 mA $cm^{-2}$. In the next step, behavior was similar to the previous step in which the electrode was responsive to addition of fresh medium. This is due to the capability of the electrode as the final electron acceptor for SRBs. From Fig. 10, it can be concluded that the active biofilm was effective as a final electron acceptor. Fig. 11 shows that fluorescence analysis corresponding to this experiment confirmed that biofilm formed on the surface has a crucial effect on the electron donor as well as potential. Biofilm (including living and dead cells in this case) formed on the surface was very responsive to increased carbon source at different periods of time. For instance, accumulation of bacteria on the surface increased at the twentieth day as compared to the first day, which indicates good adhesion of bacteria on the electrode. The density of bacteria on the surface on the thirtieth day continued to effectively increase. This continuous layer of bacteria is ready to receive additional carbon source for metabolic activity and transfer of electrons to the surface for current generation.

## 4. Conclusion

In this study, a modified stainless-steel 304 based electrode coated with activated carbon and graphite solution was employed as an expedient option in MFC technology. The results affirm that key parameters such as long-term stability of cells attachment and living cell number are more efficient in the SsCG electrode as compared to other commercial electrodes (CP and GR). A current generation of 2.26 mA obtained for the modified structure was higher than the 1.73 mA and 1.29 mA for GR and CP in the presence of SRBs in culture media. This new

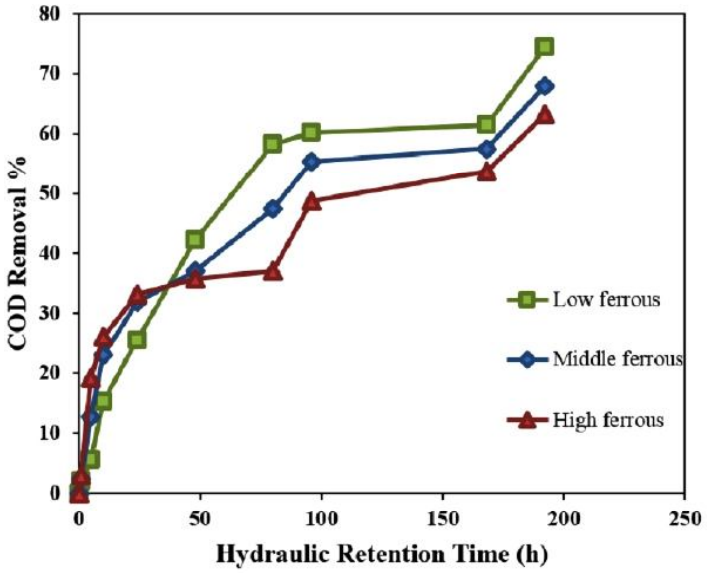


**Fig. 9. Chemical oxygen demand (COD) removal of culture mediums in different concentrations of sulfate ferrous vs. HRT.**

approach to increase bacterial population was studied with the use of two electron acceptors of iron and sulfate for respiration of SRB. The results show that maximum growth was obtained at
48 h with 1 g $dm^{-1}$ $FeSO_4$ concentration which had $n_M = 20\times10^8$ cell $ml^{-1}$ living cells. It is also revealed that there is a significant interaction between the sulfate/$Fe^{+2}$ concentrations and chemical oxygen demand (COD) on the bacterial population. The outcome of the present work is crucial for the development of processes where MFC is utilized for sulfate and COD removal as well as bioelectricity generation using SRBs.

## Acknowledgment

Financial support from the research department of Tarbiat Modares University for supporting this research work is gratefully acknowledged.

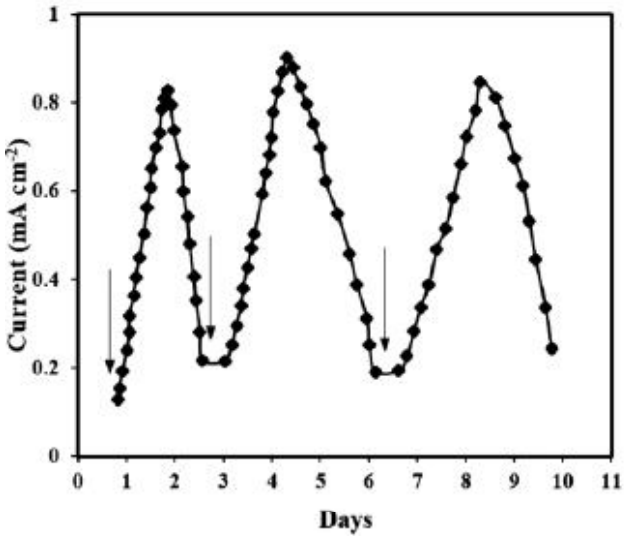


**Fig.10. Continuous current generation with decrease in sodium lactate concentration of the medium (arrow indicates reinjection of sodium lactate).**

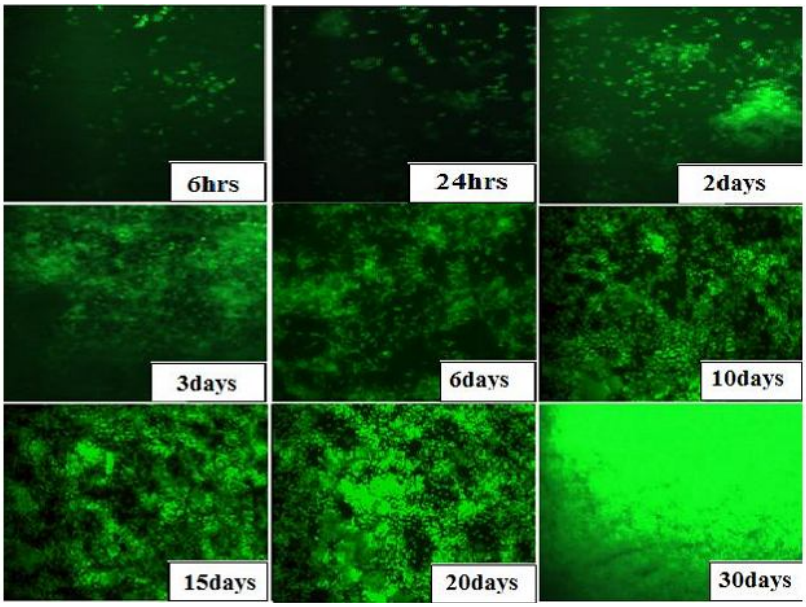


**Fig.11. Aggregation of cells and biofilm formation on anode surface of stainless steel coated with carbon solution in various periods of time.**

## References

[1] Rezaei F, Xing D, Wagner R, Regan JM, Richard TL, Logan BE., "Simultaneous cellulose degradation and electricity production by Enterobacter cloacae in a microbial fuel cell", Appl. Environ. Microbiol., 2009, 75:3673.

[2] Fraiwan A, Mukherjee S, Sundermier S, Lee H-S, Choi S., "A paper-based microbial fuel cell: Instant battery for disposable diagnostic devices", Biosens. Bioelectron., 2013, 49:410.

[3] Logan BE, Hamelers B, Rozendal R, Schröder U, Keller J, Freguia S, et al., "Microbial fuel cells: methodology and technology", Environ. Sci. Technol., 2006, 40:5181.

[4] Liu H, Ramnarayanan R, Logan BE., "Production of electricity during wastewater treatment using a single chamber microbial fuel cell", Environ. Sci. Technol., 2004, 38:2281.

[5] Gibson GR, Macfarlane G, Cummings J., "Sulphate reducing bacteria and hydrogen metabolism in the human large intestine", Gut., 1993, 34:437.

[6] Odom J., "Industrial and Environmental concerns with sulfate-reducing bacteria", ASM News (Washington), 1990, 56:473.

[7] Ghazy E, Mahmoud M, Asker M, Mahmoud M, Abo Elsoud M, Abdel Sami M., "Cultivation and detection of sulfate reducing bacteria (SRB) in sea water", J. of American Sci., 2011, 7:604.

[8] Otero JJG., "Epidemiology of marine toxins", Seafood and Freshwater Toxins: Pharmacology, Physiology, and Detection, 2014:123.

[9] Peng C-G, Park JK, Patenaude RW., "Statistics-based classification of microbially influenced corrosion in freshwater systems", Water Res., 1994, 28:95.

[10] Gerardi MH., "Sulfur-Oxidizing and Sulfur-Reducing Bacteria", Wastewater Bacteria, 2006, 117:31.

[11] Nordstrom DK., "The effect of sulfate on aluminum concentrations in natural waters: some stability relations in the system $Al_2O_3$-$SO_3$-$H_2O$ at 298 K", Geochim. Cosmochim. Acta, 1982, 46:681.

[12] Sun M, Tong Z-H, Sheng G-P, Chen Y-Z, Zhang F, Mu Z-X, et al., "Microbial communities involved in electricity generation from sulfide oxidation in a microbial fuel cell", Biosens. Bioelectron., 2010, 26:470.

[13] Zhao F, Rahunen N, Varcoe JR, Chandra A, Avignone-Rossa C, Thumser AE, et al., "Activated carbon cloth as anode for sulfate removal in a microbial fuel cell", Environ. Sci. Technol., 2008, 42:497.

[14] Clauwaert P, Aelterman P, De Schamphelaire L, Carballa M, Rabaey K, Verstraete W., "Minimizing losses in bio-electrochemical systems: the road to applications", Appl. Microbiol. Biotechnol., 2008, 79:901.

[15] Logan BE., "Exoelectrogenic bacteria that power microbial fuel cells", Nat. Rev. Microbiol., 2009, 7:375.

[16] Zhou M, Chi M, Luo J, He H, Jin T., "An overview of electrode materials in microbial fuel cells", J. Power Sources., 2011, 196:4427.

[17] Hindatu Y, Annuar M, Gumel A., "Mini-review: Anode modification for improved performance of microbial fuel cell", Renewable Sustainable Energy Rev., 2017, 73:236.

[18] Jia N, Wang Z, Yang G, Shen H, Zhu L., "Electrochemical properties of ordered mesoporous carbon and its electroanalytical application for selective determination of dopamine", Electrochem. Commun., 2007, 9:233.

[19] Postgate J., "Differential media for sulphur bacteria", J. Sci. Food Agric., 1959, 10:669.

[20] Nevin KP, Richter H, Covalla S, Johnson J, Woodard T, Orloff A, et al., "Power output and columbic efficiencies from biofilms of Geobacter sulfurreducens comparable to mixed community microbial fuel cells", Environ.

Microbiol., 2008, 10:2505.

[21] Stadler R, Fuerbeth W, Harneit K, Grooters M, Woellbrink M, Sand W., "First evaluation of the applicability of microbial extracellular polymeric substances for corrosion protection of metal substrates", Electrochimica Acta, 2008, 54:91.

[22] McKane L, Kandel J., "Bacterial Growth and Laboratory Cultivation", Microbiology Essentials and Applications New York: McGraw-Hill, Inc., 1996, 97:125.

[23] Cord-Ruwisch R., "A quick method for the determination of dissolved and precipitated sulfides in cultures of sulfate-reducing bacteria", J. Microbiol. Methods, 1985, 4:33.

[24] Karamanev D, Nikolov L, Mamatarkova V., "Rapid simultaneous quantitative determination of ferric and ferrous ions in drainage waters and similar solutions", Miner. Eng., 2002, 15:341.

[25] Zhao F, Wu X, Wang M, Liu Y, Gao L, Dong S., "Electrochemical and bioelectrochemistry properties of room-temperature ionic liquids and carbon composite materials", Anal. Chem., 2004, 76:4960.

[26] Aelterman P, Versichele M, Marzorati M, Boon N, Verstraete W., "Loading rate and external resistance control the electricity generation of microbial fuel cells with different three-dimensional anodes", Bioresour. Technol., 2008, 99:8895.

[27] Rabaey K, Verstraete W., "Microbial fuel cells: novel biotechnology for energy generation", Trends Biotechnol., 2005, 23:291.

[28] Herrera LK, Videla HA., "Role of iron-reducing bacteria in corrosion and protection of carbon steel", Int. Biodeterior. Biodegrad., 2009, 63:891.

[29] Lopes F, Morin P, Oliveira R, Melo L., "Interaction of Desulfovibrio desulfuricans biofilms with stainless steel surface and its impact on bacterial metabolism", J. Appl. Microbiol., 2006, 101:1087.

[30] Lovley DR, Coates JD, Blunt-Harris EL, Phillips EJ, Woodward JC., "Humic substances as electron acceptors for microbial respiration" Nature, 1996, 382:445.

[31] Lovley DR, Phillips EJ., "Competitive mechanisms for inhibition of sulfate reduction and methane production in the zone of ferric iron reduction in sediments", Appl. Environ. Microbiol., 1987, 53:2636.

[32] Castro HF, Williams NH, Ogram A., "Phylogeny of sulfate-reducing bacteria", FEMS Microbiology Ecology, 2000, 31:1.

[33] Hashemi J, Samimi A., "Steady state electric power generation in up-flow microbial fuel cell using the estimated time span method for bacteria growth domestic wastewater", Biomass and bioenergy, 2012, 45:65.

[34] Singh R, Kumar A, Kirrolia A, Kumar R, Yadav N, Bishnoi NR, et al., "Removal of sulphate, COD and Cr (VI) in simulated and real wastewater by sulphate reducing bacteria enrichment in small bioreactor and FTIR study", Bioresour. technol., 2011, 102:677.

[35] Song YC, Kim DS, Woo JH, Subha B, Jang SH, Sivakumar S., "Effect of surface modification of anode with surfactant on the performance of microbial fuel cell", Int. J. Energy Res., 2015, 39:860.

[36] Hou J, Liu Z, Yang S, Zhou Y., "Three-dimensional macroporous anodes based on stainless steel fiber felt for high-performance microbial fuel cells", J. Power Sources, 2014, 258:204.

[37] Zheng S, Yang F, Chen S, Liu L, Xiong Q, Yu T, et al., "Binder-free carbon black/stainless steel mesh composite electrode for high-performance anode in microbial fuel cells", J. Power Sources, 2015, 284:252.

[38] Guo K, Donose BC, Soeriyadi AH, Prévoteau A, Patil SA, Freguia S, et al., "Flame oxidation of stainless steel felt enhances anodic biofilm formation and current output

in bioelectrochemical systems", Environ. Sci. Technol., 2014, 48:7151.

[39] Lamp JL, Guest JS, Naha S, Radavich KA, Love NG, Ellis MW, et al., "Flame synthesis of carbon nanostructures on stainless steel anodes for use in microbial fuel cells", J. Power Sources, 2011, 196:582.

[40] Erbay C, Pu X, Choi W, Choi M-J, Ryu Y, Hou H, et al., "Control of geometrical properties of carbon nanotube electrodes towards high-performance microbial fuel cells", J. Power Sources, 2015, 280:347.